COMPARISON OF MODEL VS. REALITY FOR VELA

M. S. Toplis, J. W. McKenzie, B. D. Muratori, D. J. Scott, P. H. Williams*
STFC Daresbury Laboratory & Cockcroft Institute, Warrington, UK

Abstract

The Versatile Electron Linear Accelerator (VELA) is a facility designed to provide a high quality electron beam for accelerator systems development, as well as industrial and scientific applications. Currently, the RF gun can deliver short bunches, of the order of 100 fs to a few ps, with a charge of up to 250 pC, at the longer bunch lengths, and up to 4.5 MeV/c beam momentum. A model for the injector has been developed in ASTRA, together with a suite of scripts to create scans of the available parameters around an empirically found arbitrarily optimal working point. The space of parameters consists of everything that can be changed in the control room, and ranges from bunch charge to laser spot size on the cathode, together with all magnet settings where and if necessary. The various scans facilitate the task of identifying where exactly the accelerator is in terms of parameters and trends. Initial comparisons of screen images are made between the model and reality. Ultimately, the goal of the model is to robustly and repeatably establish a desired operating setup on a daily basis from an unknown switch on condition.

MACHINE CONDITIONS & DATA TAKING

A full description of the VELA facility and its development to date can be found in [1]. Here we concentrate on the beam dynamics in the 3 m directly following the cathode. The layout of the relevant section is shown in Fig. 1.

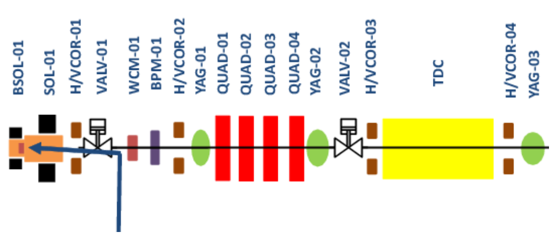

Figure 1: Layout of the first 3 m of VELA.

As this experiment is intended to be an initial step in establishing an automated procedure to set up the entire machine, it was decided to simplify the setup as much as practicable. To this end, the bucking coil in the gun (BSOL-01), all correctors and the four quadrupoles situated in the section under study were degaussed and switched off, as was the transverse deflecting cavity (TDC). The remaining variable machine settings were therefore the gradient and phase of the RF in the gun cavity, the field strength of the main solenoid (SOL-01), the intensity of the laser spot and the position of the laser spot on the cathode, observed on a virtual cathode. To further simplify, we chose to fix the gradient and phase of the gun to the empirically established operational nominal that produces beam of momentum 4.5 MeV/c at an off-crest phase of -15 degrees (where negative indicates the laser pulse follows after the RF crest). This was set using a previously calibrated beam position in a BPM located in a spectrometer line just beyond YAG-03 when the spectrometer dipole is excited to a particular known field. The accuracy and precision of these settings is noted for later variation in the model to help establish the likely true values. The beam was then centered in the gun cavity and solenoid by observing its movement on YAG-03 as the gun phase and solenoid current were adjusted. Therefore no assumption is made that virtual cathode relative positions and laser spot sizes correspond to those on the real cathode.

A scan was then performed as follows: at each of the three screens indicated in Fig. 1, five images were recorded on consecutive shots at 10 Hz and timestamped, together with five background images again from consecutive shots at 10 Hz with the laser shutter closed. This was performed for four charge settings: 2 pC, 20 pC, 50 pC and 100 pC. Camera gains were adjusted such that no pixel was saturated at the highest bunch charge and it was confirmed that images well above background were still seen at the lowest charge. This procedure was then repeated for four corners of a square on the virtual cathode, approximately: (-0.5, -2), (-1.5, -2), (-1.5, -1) and (-0.5, -1), where (X,Y) positions are given in mm and determined by referring to the 0.5 mm graticule markings on the virtual cathode. The centre as determined above is the first point.

During data taking several parameters were continuously recorded with timestamps to monitor drifts in the RF system and establish bunch charge error, namely:

1. Gun and klystron forward and reverse powers
2. Electron bunch charge as measured by the wall current monitor (WCM-01) indicated in Fig. 1
3. Temperature of the gun cavity water cooling system
4. Beam positions as measured on stripline BPMs in the horizontal and vertical plane

IMAGE ANALYSIS

A standardised image analysis procedure has been defined for VELA [2]. Each image is preprocesed thus:

1. Background subtracted to reduce dark current
2. Image cut to screen surface using an elliptical mask
3. Normal distributions fit to the image projections
4. Fits used to cut the image to 3σ in X and Y either side of the mean position
5. Saturated points removed

* peter.williams@stfc.ac.uk

After pre-processing a mean vector and covariance matrix defined by the X and Y variances σ_{xx}, σ_{yy} and the XY covariance σ_{xy} are extracted using two methods: least squares fitting of a bivariate normal distribution (BVN) or by direct calculation using binned maximum likelihood estimation (MLE). Errors were estimated as simply the standard deviation of the beam sizes of the five consecutive images taken, which dominates over any fit residuals. The results of both methods are shown in Fig. 2.

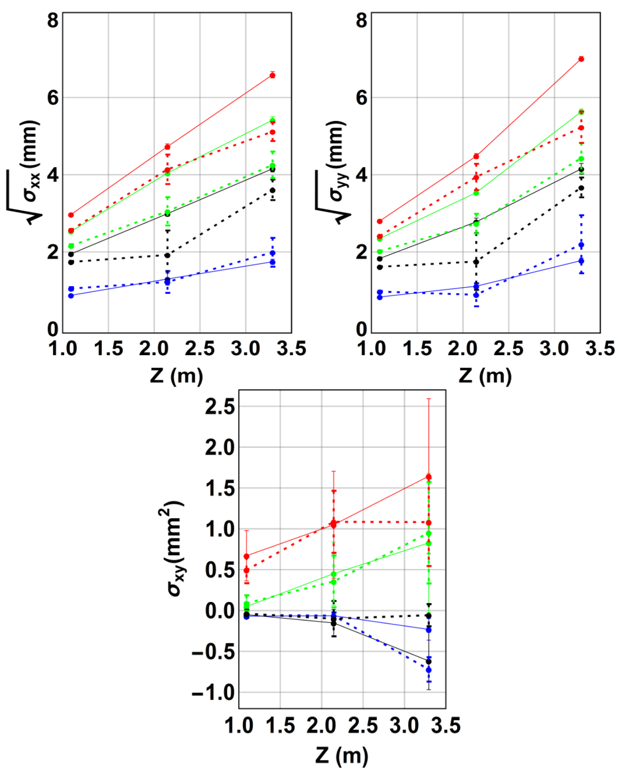

Figure 2: Calculated $\sqrt{\sigma_{xx}}$ (horizontal beam size), $\sqrt{\sigma_{yy}}$ (vertical beam size) and σ_{xy} (ellipse interaxis correlation - indicating tilt angle) from images at YAG-01, YAG-02 and YAG-03 (indicated at their true distances from the cathode). Four bunch charges are shown: 2 pC (blue), 20 pC (black), 50 pC (green) and 100 pC (red). For each two sets of data are shown: solid lines depict when the images have been analysed using the BVN method, dashed lines indicate MLE method.

It was found that the BVN method is better able to reject background image noise in its fit, but it takes longer than the MLE method.

MACHINE SIMULATIONS

A simulation of the machine was developed from the design model constructed in ASTRA [3]. A suite of scripts automates the process of generating parameter scans through multiple runs. For each of the machine conditions for which data was taken a scan was performed where the fixed parameters were varied to establish the likeliest true values, these variables are shown in Table 1.

Table 1: Simulation parameters varied. Nominal, minimum, maximum and stepsize are shown. From left to right the parameters are: thermal emittance, rms laser spot size, gun gradient, gun phase and solenoid strength.

Param.	ε_{th}	R_{laser}	E_{gun}	ϕ_{gun}	B_{sol}
Unit	eV	mm	MV/m	°	T
Nom.	0.62	0.15	70	-15	0.20
Min	0.42	0.11	64	-21	0.14
Max	0.82	0.19	76	-9	0.26
Step	0.1	0.02	3	3	0.03

Due to time constraints simulations were only generated with centrally fixed laser spot position and only data where the beam was centred in the gun and solenoid was used. Additionally, the full analysis presented here is only for the 50 pC case.

In order to avoid the introduction of systematic bias, our original intention was to extract positional distributions at the screens from each ASTRA simulation, bin them into pixels and subject them to the image analysis in an identical way to the images from the machine. However, the large beam sizes that can occur at the edges of our parameter space are computationally expensive when the BVN method is used. Additionally, the small number of macroparticles necessitated by the requirement of many thousands of separate scans leads to granularity that the BVN method is unable to fit to accurately.

For our analysis we therefore only treated the simulated images with an unbinned MLE method. This is fast and also not affected by granularity. However it is no longer obvious how to compare this with the real images, we therefore show the results of both methods of analysis on the real images. Errors shown on the simulated images are purely statistical.

ANALYSIS & RESULTS

As all simulations were conducted with 1000 macroparticles, a convergence study was performed to assess whether the errors thus introduced are dominant. Figure 3 shows that the beam size values extracted from ASTRA at 1000 macroparticles are within 10% of those when 500,000 are tracked.

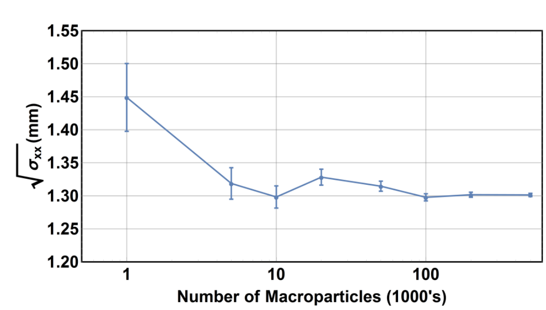

Figure 3: Log plot of simulated horizontal beam size at YAG-01 in an indicative ASTRA simulation as a function of number of macroparticles tracked.

ISBN 978-3-95450-147-2

The closeness of each simulation to the machine images was then estimated by performing a Welch's t-test [4, 5] on the data pairs corresponding to each screen. This can be viewed as equivalent to the construction of a penalty function for minimisation in a standard accelerator physics design optimisation. Thus we are able to determine a small number (preferably one) of simulation parameter sets that best fit the observed conditions. It should be emphasised that this is not an optimisation, but an assessment of the best fit against pregenerated sets of simulations.

Fig. 4 shows comparisons of the best and worst fitting ASTRA distributions to the machine images for beam sizes along the X axis.

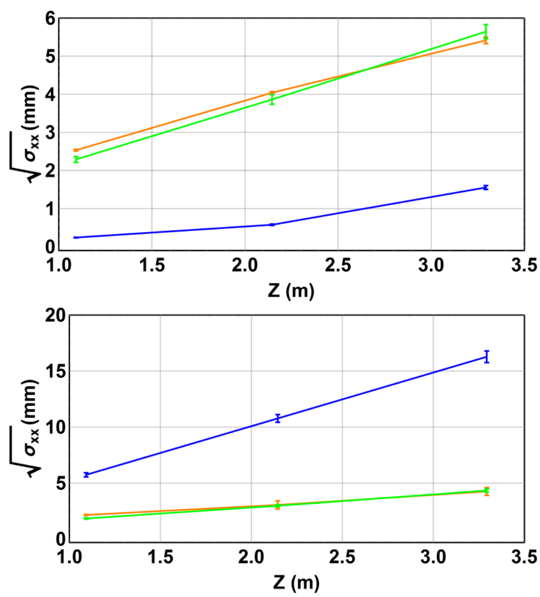

Figure 4: Comparisons of the best and worst fitting ASTRA distributions in X. $\sqrt{\sigma_{xx}}$ from the machine images is shown in orange, the best fitting ASTRA distribution is shown in green and the worst fitting ASTRA distribution is shown in blue. The top plot shows the comparison of machine images analysed using the BVN method, the bottom plot shows machine images analysed using the MLE method.

The best fitting parameters are given for both methods of analysis on the X and Y beam sizes in Table 2.

Table 2: Best fit results in X and Y from each method for the 50 pC case. These parameter sets give the minimum penalty function value in each case, so give the closest fits to the images taken from the machine.

Param.	ε_{th}	R_{laser}	E_{gun}	ϕ_{gun}	B_{sol}
Unit	eV	mm	MV/m	°	T
Nom.	0.62	0.15	70	-15	0.20
BVN X	0.42	0.11	70	-15	0.20
BVN Y	0.42	0.19	70	-15	0.20
MLE X	0.52	0.13	67	-21	0.20
MLE Y	0.62	0.19	67	-21	0.20

Figure 5 shows the calculated penalty function for each of the simulations at 50 pC with the laser spot centred on the cathode. Progressive zooming in shows indicative variation under each parameter considered.

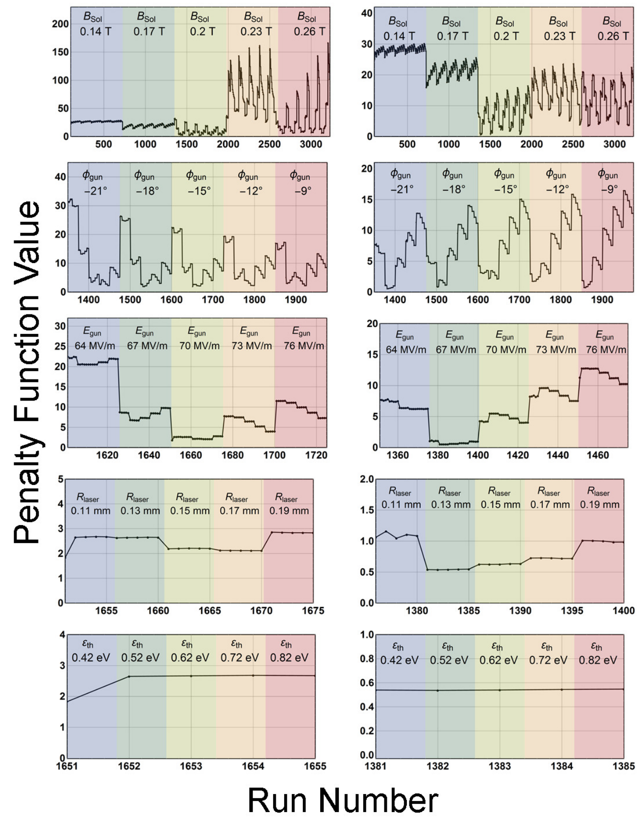

Figure 5: Penalty function progressively zoomed at the minimum parameter to show indicative variation under each variable considered. Images analysed using the BVN method (left column) and the MLE method (right column) for beam sizes along the X axis. Each row shows the minimum segment of the plot above it, as can be seen by looking at the run numbers on the horizontal axis.

CONCLUSIONS & FUTURE DEVELOPMENTS

It should be understood that this is an initial exploration of this method, and results should be treated with caution at this stage. Nevertheless we are encouraged in that the nominal predicted values are in reasonable agreement with the real data. Our results suggest that the gun gradient is close to what we anticipated for this beam momentum but the laser spot size is different to that inferred from the virtual cathode images, the gun phase differs slightly depending on the analysis method used but is equal to the nominal for the BVN and the fits point to smaller thermal emittances than expected.

The intention is to expand this approach to more complex machine configurations with more variables. Additionally, we will fully automate the procedure and incorporate into machine learning algorithms to achieve an accelerator that optimises itself with no requirement for human intervention.

REFERENCES

[1] D.J. Scott et al., THPOW019, these proceedings

[2] M.S. Toplis & D.J. Scott, "Method of Estimating Beam Size from VELA Screen Images", unpublished

[3] K. Floettmann, ASTRA - A Space Charge Tracking Algorithm, `http://www.desy.de/~mpyflo/`

[4] B.L. Welch, "The generalization of "Student's" problem when several different population variances are involved", Biometrika, 1947, vol 34 (1-2): 28-35

[5] G.D. Ruxton, "The unequal variance t-test is an underused alternative to Student's t-test and the Mann-Whitney U test", Behavioral Ecology, 2006, vol 17 (4): 688-690

ISBN 978-3-95450-147-2